

PDF hosted at the Radboud Repository of the Radboud University Nijmegen

The following full text is a publisher's version.

For additional information about this publication click this link.

<http://hdl.handle.net/2066/34563>

Please be advised that this information was generated on 2019-02-19 and may be subject to change.

Traditional Biomolecular Structure Determination by NMR Spectroscopy Allows for Major Errors

Sander B. Nabuurs¹, Chris A. E. M. Spronk¹, Geerten W. Vuister^{2*}, Gert Vriend^{1*}

1 Center for Molecular and Biomolecular Informatics, Nijmegen Center for Molecular Life Sciences, Radboud University, Nijmegen, Netherlands, **2** Department of Biophysical Chemistry, Institute for Molecules and Materials, Radboud University, Nijmegen, Netherlands

One of the major goals of structural genomics projects is to determine the three-dimensional structure of representative members of as many different fold families as possible. Comparative modeling is expected to fill the remaining gaps by providing structural models of homologs of the experimentally determined proteins. However, for such an approach to be successful it is essential that the quality of the experimentally determined structures is adequate. In an attempt to build a homology model for the protein dynein light chain 2A (DLC2A) we found two potential templates, both experimentally determined nuclear magnetic resonance (NMR) structures originating from structural genomics efforts. Despite their high sequence identity (96%), the folds of the two structures are markedly different. This urged us to perform in-depth analyses of both structure ensembles and the deposited experimental data, the results of which clearly identify one of the two models as largely incorrect. Next, we analyzed the quality of a large set of recent NMR-derived structure ensembles originating from both structural genomics projects and individual structure determination groups. Unfortunately, a visual inspection of structures exhibiting lower quality scores than DLC2A reveals that the seriously flawed DLC2A structure is not an isolated incident. Overall, our results illustrate that the quality of NMR structures cannot be reliably evaluated using only traditional experimental input data and overall quality indicators as a reference and clearly demonstrate the urgent need for a tight integration of more sophisticated structure validation tools in NMR structure determination projects. In contrast to common methodologies where structures are typically evaluated as a whole, such tools should preferentially operate on a per-residue basis.

Citation: Nabuurs SB, Spronk CAEM, Vuister GW, Vriend G (2006) Traditional biomolecular structure determination by NMR spectroscopy allows for major errors. *PLoS Comput Biol* 2(2): e9.

Introduction

Experimentally determined three-dimensional structures of biomolecules form the foundation of structural bioinformatics, and any structural analysis would be impossible without them. Two main techniques are available for biomolecular structure determination: x-ray crystallography and nuclear magnetic resonance (NMR) spectroscopy. It is important to realize that all resulting structure models are derived from their underlying experimental data. Unfortunately, any experiment and thus any structure model will have errors associated with it. Random errors depend on the precision of the experimental measurements and are propagated to the precision of the final models. Systematic errors and mistakes often result from errors in the interpretation of the experimental data and relate directly to the accuracy of the final structure models. For example, in NMR spectroscopy errors can be introduced by misassignment of the spectral signals; in x-ray crystallography errors are most likely made when the protein structure is positioned in the electron density [1,2].

Several studies have shown that not all experimentally determined biomolecular structure models are of equally high quality [3–6]. Many different types of errors can be identified in protein structures, ranging from too tightly restrained bond lengths and angles, to molecules exhibiting a completely incorrect fold. Where the former type of errors often does not have large consequences for the analysis of the

structure and typically can be easily remedied by refinement in a proper force field [7,8], the latter renders a structure model completely useless for all practical purposes. Throughout the years several such errors have been uncovered in the Protein Data Bank (PDB) [9], which often resulted in the replacement of the incorrect models with improved ones.

A typical example of an incorrectly folded structure model is the first crystal structure of photoactive yellow protein. The structure was solved initially in 1989 [10] and deposited under the now obsolete PDB entry 1PHY. An updated model released 6 y later showed that in the original model the electron density had been misinterpreted [11] (PDB entry 2PHY). Similar chain tracing problems led to an incorrect

Editor: Philip Bourne, University of California San Diego, United States of America

Received: September 28, 2005; **Accepted:** December 29, 2005; **Published:** February 3, 2006

A previous version of this article appeared as an Early Online Release on December 29, 2005 (DOI: 10.1371/journal.pcbi.0020009.eor).

DOI: 10.1371/journal.pcbi.0020009

Copyright: © 2006 Nabuurs et al. This is an open-access article distributed under the terms of the Creative Commons Attribution License, which permits unrestricted use, distribution, and reproduction in any medium, provided the original author and source are credited.

Abbreviations: DLC2A, dynein light chain 2A; NMR, nuclear magnetic resonance; NOE, nuclear Overhauser enhancement; PDB, Protein Data Bank; RDC, residual dipolar coupling

* To whom correspondence should be addressed. E-mail: G.Vuister@science.ru.nl (GWV); G.Vriend@cmbi.ru.nl (GV)

Synopsis

Three-dimensional biomolecular structures provide an invaluable source of biologically relevant information. To be able to learn the most of the wealth of information that these structures can provide us, it is of great importance that the quality and accuracy of the protein structure models deposited in the Protein Data Bank are as high as possible. In this work, the authors describe an analysis that illustrates that this is unfortunately not the case for many protein structures solved using nuclear magnetic resonance spectroscopy. They present an example in which two strikingly different models describing the same protein are analyzed using commonly available structure validation tools, and the results of this analysis show one of the two models to be incorrect. Subsequently, using a large set of recently determined structures, the authors demonstrate that unfortunately this example does not stand on its own. The analyses and examples clearly illustrate that relying solely on the experimental data to evaluate structural quality can provide a false sense of correctness and the combination of multiple sophisticated structure validation tools is required to detect the presence of errors in protein nuclear magnetic resonance structures.

model for a DD-peptidase [12] (the now obsolete PDB entry 1PTE), which was corrected 10 y later when the structure was solved again but now at higher resolution [13] (PDB entry 3PTE).

Also, for structures determined using NMR spectroscopy, cases are known where reevaluation of the experimental data, often prompted by publication of a corresponding structure, has resulted in the replacement of structures in the PDB. A well-known example is the original NMR structure of the oligomerization domain of p53 [14]. In this dimer of dimers, a difference in the orientation of the two dimers was observed between the NMR and crystal structure, the latter published shortly after the NMR structure [15] (PDB entry 1C26). Reexamination of the nuclear Overhauser enhancement (NOE) data led to the identification of three misinterpreted peaks in the original p53 NOE assignments and the inclusion of several new NOEs, resulting in a revision of the original PDB entry [16] (PDB entry 1OLH). A similar low number of misinterpreted NOE signals (17 in total) resulted in a largely incorrect fold for the anti- σ factor AsiA [17] (the now obsolete PDB entry 1KA3). In this case, it was not until a second solution structure of AsiA was published [18] (PDB entry 1JR5) that the experimental data of the original AsiA structure were reexamined and the assignment errors were discovered [19] (updated PDB entry 1TKV).

In this paper, we describe a detailed analysis of two recently released NMR structures of the protein dynein light chain 2A (DLC2A), one from human (PDB entry 1TGQ) and one from mouse (PDB entry 1Y4O). Both structures originate from large structural genomics initiatives: the structure of human DLC2A (hDLC2A) was determined by the Northeast Structural Genomics Consortium (NESGC, <http://www.nesg.org>), and the mouse variant (mDLC2A) was determined by the Center for Eukaryotic Structural Genomics (CESG, <http://www.uwstructuralgenomics.org>). Despite 96% sequence identity, large structural differences are observed between the two ensembles; an unexpected and extremely unlikely result. Using the deposited experimental data we show that only the 1Y4O structure ensemble is correct. Subsequently, we analyze both ensembles using various structure and data validation

methods to show that the erroneous structure ensemble could have been identified prior to deposition. Finally, we validate a large set of protein NMR structures that were released from the PDB in the period 2003 to 2005 and show that the DLC2A example does not stand on its own, but that more errors of this magnitude can be found. We conclude with some suggestions on how, in the future, such large errors can be identified during the structure determination process using readily available validation software.

Results/Discussion

Our interest in DLC2A originated from a request by one of our collaborators to build a homology model for this protein. A BLAST search in February 2005 [20] against the PDB revealed that construction of a homology model should be straightforward: two NMR structures of DLC2A (PDB entries 1Y4O and 1TGQ), both with more than 95% sequence identity to the target sequence, had been released in the months prior to our query. Surprisingly, a first visual inspection of both structures revealed striking differences, as shown in Figure 1.

It is immediately obvious that DLC2A forms a dimer in the 1Y4O structure models (Figure 1C), whereas the 1TGQ ensemble contains DLC2A in monomeric form (Figure 1D). Additionally, the DLC2A models feature remarkably different folds. The central α -helix ($\alpha 2$ in Figure 1A and 1B), which extends from Asn44 to Ile68 in the 1Y4O ensemble, consists in the 1TGQ ensemble of two separate, almost antiparallel, α -helices (Thr46-Ser52 and Phe57-Thr64) connected by a turn-like region (Leu53-Ser56). Beta strands $\beta 3$ (Leu71-Ser80) and $\beta 4$ (Glu85-Pro90) pack tightly against each other in the 1Y4O structure models. In the 1TGQ structures, the $\beta 3$ region forms a hairpin-like structure, and the $\beta 4$ strand is much less tightly packed against the core of the protein.

During evolution, protein structure has always been more stable and has changed much slower than the associated sequence [21]. As a result, similar sequences fold into practically identical structures and remotely related sequences still adopt similar folds [22]. An accurate limit for this rule was recently derived by Rost [23], who found that two sequences that share over 30% sequence identity in 100 aligned residues are practically guaranteed to have the same fold. Given this knowledge, it is extremely unlikely for mouse and human DLC2A, which share 96% sequence identity, to fold into the different structures shown in Figure 1C and 1D.

Visual inspection of the two ensembles made us realize quickly that the large differences probably originate from the oligomeric state of the two structures. Using NMR spectroscopy (and in most structural genomics initiatives [24]), the presence of tertiary structure in a soluble protein is typically assessed using a proton-nitrogen correlation (^{15}N -HSQC) spectrum [25]. The observed pattern of dispersed signals, ideally one for each amino acid, provides a “fingerprint” of the protein. However, the formation of a symmetric dimer, as shown in Figure 1A, does not result in a doubling of the number of observed NMR signals. Consequently, it is not straightforward to determine the oligomeric state of a protein from its ^{15}N -HSQC NMR spectra alone, and typically assessments have to be made from estimates of the protein's relaxation rates [26]. Therefore, if the oligomeric state of a protein is not known or is incorrectly known, the NMR

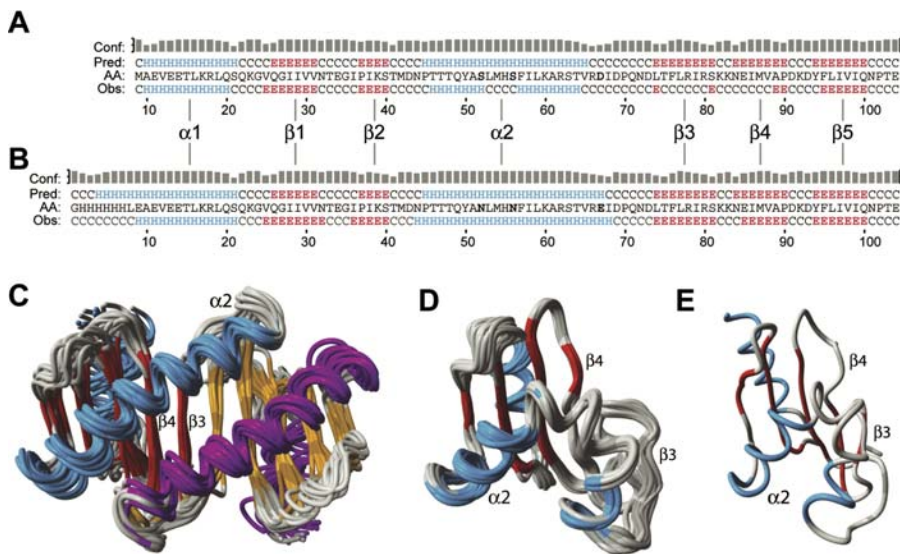


Figure 1. Sequence and Structure Ensembles of Two DLC2A Structures

(A) The sequence of human DLC2A (hDLC2A) (AA).

(B) The sequence of mouse DLC2A (mDLC2A) proceeded by an eight-residue His-tag (AA). The secondary structure as predicted using PSIPRED [33,50] (Pred) and the confidence of this prediction (Conf) are shown above the sequences. The secondary structure as observed in the ensembles (Obs) is indicated below the sequences. Except for the His-Tag, the mouse and human sequences differ at three positions (indicated in bold).

(C) Ribbon diagram of the structure ensemble of mDLC2A (PDB entry 1Y4O). The residues of the His-tag have been omitted for clarity.

(D) Ribbon diagram of the structure ensemble of hDLC2A (PDB entry 1TGQ).

(E) The refined average structure of the ensemble calculated using the reconstructed 1TGQ dataset, as discussed in the text. Secondary structure is indicated using colors: helices are shown in blue and purple, strands are shown in red and orange. A numbering scheme for the secondary structure elements is indicated between the two sequences.

DOI: 10.1371/journal.pcbi.0020009.g001

spectra of a dimeric protein could be easily interpreted as originating from a monomer. Below, we present evidence that such a misinterpretation is the root-cause of the observed differences between the human and mouse DLC2A structure ensembles.

Figure 1C shows that the two α 2-helices in the dimer interface are oriented in an antiparallel fashion. As a result, intermolecular signals arising from, for example, contacts between the N-terminal and C-terminal sides of these respective helices are to be expected. When it is a priori known that the protein under investigation is a dimer, specific experiments can be performed to distinguish such intermolecular contacts from the intramolecular ones [27]. However, if the intermolecular contacts are wrongly interpreted as intramolecular, the residues involved would appear to be close to each other also in the monomeric structure, something that is indeed observed in the structure models shown in Figure 1D.

To further test this hypothesis, we used the experimental NMR restraints from the 1Y4O structure ensemble (as those for the 1TGQ ensemble were not available) and changed all 72 intermolecular NOEs into 36 intramolecular distance restraints. With this simulated subset of 36 erroneous intramolecular NOEs (hereafter referred to as the 1TGQ_{sim} dataset) and the experimentally observed intramolecular restraints, structure calculations were performed. An ensemble of 20 structures without any distance violations larger than 0.5 Å was readily obtained. The refined geometric average of this ensemble is shown in Figure 1E, and it exhibits a fold very similar to that observed for the 1TGQ ensemble. These results provide a strong indication that the NMR spectra of hDLC2A were indeed interpreted as those of a

monomer, while the protein, like its mouse homolog, is actually a dimer in solution. Conclusive evidence that the human DLC2A protein does indeed form a dimer was obtained from the NESGC Web site, where the aggregation screening records associated with hDLC2A clearly show that this protein forms dimers in solution (http://spine.nesg.org/buffer_exchange.pl?id=HR2106). During the reviewing process of this paper, one of the referees pointed us to the publication of an independent structure determination of the human homolog in August 2005 (PDB entry 1Z09) [28], which was indeed also solved as a dimer. Subsequently, in November 2005, 1.5 y after its original deposition, the monomeric PDB entry 1TGQ was replaced by a correct dimeric structure (PDB entry 2B95).

Data and Structure Analyses

Having established the origin of the errors present in the 1TGQ ensemble, we can now ask the most important question: Could these errors have been discovered during the structure determination and validation process? To investigate this issue, the deposited structure ensembles were evaluated using common structure validation tools. In addition, both structure ensembles were refined in explicit solvent [7,8] and subsequently also included in the structure validation process. The DLC2A models of the 1Y4O ensemble were refined against the deposited NOE distance restraints and dihedral angle restraints. As mentioned before, for the 1TGQ ensemble no experimental restraints had been deposited, and therefore the intramolecular restraints as obtained from the 1Y4O dataset were used. In addition, the restraints from the 1TGQ_{sim} dataset were also included in the refinement of the 1TGQ structures. The structure validation

Table 1. Average Quality Indicators of the 1Y4O and 1TGQ Structure Ensembles before and after Refinement in Explicit Solvent

Criteria	Characteristic	1Y4O (Original)	1Y4O (Refined)	1TGQ (Original)	1TGQ (Refined)
Agreement with experimental data	RMS violation 1Y4O distance restraints (Å)	0.0129	0.0097	0.607	0.0284
	Violations >0.5 Å 1Y4O distance restraints	0	0	63	0
	RMS violation 1TGQ _{sim} restraints (Å)	12.8	12.6	0.521	0.0231
	Violations >0.5 Å 1TGQ _{sim} restraints	32	32	4	0
PROCHECK validation results ^a	RMS violation 1Y4O dihedral restraints (°)	0.497	0.336	25.0	1.59
	Violations >5° 1Y4O dihedral restraints	0	0	34	4
	Most favored regions	91.2	90.5	67.7	85.8
	Additionally allowed regions	8.4	9.0	27.3	12.8
WHAT IF structure Z-scores ^b	Generously allowed regions	0.2	0.2	4.7	0.5
	Disallowed regions	0.2	0.3	0.2	0.9
	Packing quality	-0.4	0.1	-2.1	-1.5
	Ramachandran plot appearance	-3.6	-3.3	-6.6	-4.6
	χ_1/χ_2 rotamer normality	-0.3	-0.7	-5.8	-3.0
	Backbone conformation	-0.8	-1.1	-5.4	-5.4

^aPercentage of residues present in the four different regions of the Ramachandran plot.

^bA Z-score [31,32] is defined as the deviation from the average value for this indicator observed in a database of high-resolution crystal structures, expressed in units of the standard deviation of this database-derived average. Typically, Z-scores below a value of -3 are considered poor, those below -4 are considered bad.

DOI: 10.1371/journal.pcbi.0020009.t001

results for the two original and the two re-refined structural ensembles are shown in Table 1.

The 1Y4O ensemble demonstrates a good agreement with the experimentally deposited restraints. For the distance restraints, no violations larger than 0.5 Å are observed, for the dihedral angle restraints, we find no violations larger than 5°. Both these thresholds are widely considered as compatible with and representative for a good structure within the NMR community. As expected, the 1TGQ_{sim} dataset of erroneous intramolecular restraints exhibits very large violations for the 1Y4O ensembles. The validation scores, as determined by the programs PROCHECK [29] and WHAT IF [30], all fall within acceptable ranges; only the Ramachandran plot Z-score [31] of -3.3 might be considered poor [32]. Still, this score is substantially better than that of a typical NMR structure taken from the PDB [8]. The refinement in explicit solvent slightly improves the quality indicators of the 1Y4O ensemble and the agreement of the structures with the experimental data. For comparison, we also evaluated the quality of the recently released and the updated DLC2A entries in the PDB (entries 1Z09 and 2B95, respectively). Both exhibit quality scores much comparable to those of the 1Y4O ensemble, with again only the Ramachandran plot score being somewhat poor (data not shown).

The quality indicators for the deposited 1TGQ ensemble are, however, considerably worse when compared to those of the 1Y4O structure models: the majority of the quality Z-scores identify this structure as an outlier (Z-score < -4). The agreement of the original 1TGQ ensemble with the experimental restraints from 1Y4O is quite poor, but this is to be expected as these restraints were not used in the actual 1TGQ structure determination. The agreement of the 1TGQ_{sim} dataset with the 1TGQ ensemble is much better than for the 1Y4O ensemble. After a refinement in explicit solvent, the 1TGQ ensemble has accommodated to all distance restraints and does not show any violations larger than 0.5 Å. It is, however, unable to completely fulfill the experimental dihedral angle restraints of the 1Y4O dataset. On average four dihedral angle restraints per structure are violated by more than 5° in the refined 1TGQ ensemble, but none of

these violate more than 15°. The refinement results in a considerable improvement of the PROCHECK validation scores and the percentage of residues in the most favored regions of the Ramachandran plot increases to a commonly considered acceptable score of 85.8%. Most of the WHAT IF quality Z-scores improve, but both the Ramachandran plot and the backbone normality scores remain at a very worrisome level (below -4). Also the χ_1/χ_2 rotamer normality does not reach the level of quality typically observed for this quality indicator after a refinement in explicit solvent [8].

All in all, our results show that an incorrectly folded NMR structure is easily refined to a good agreement with the experimental input data and acceptable PROCHECK Ramachandran plot statistics. The overall WHAT IF quality indicators identify the structure as problematic, but only the χ_1/χ_2 rotamer normality score is significantly worse than the 100 refined structures present in the DRESS database [8]. When judged by its overall quality parameters, it is understandable, but nevertheless worrisome, that the erroneous 1TGQ ensemble went unnoticed through the structure determination and validation pipeline at the NESGC. However, a more detailed inspection of the validation results shows that the problematic regions of this ensemble of structures could have been identified.

Structure Validation on a per-Residue Basis

One of the first and very straightforward indicators that something might be wrong with the 1TGQ structure ensemble is the large discrepancy between the predicted and observed secondary structure, as shown in Figure 1A. Modern secondary structure prediction algorithms, such as the PSIPRED algorithm [33] applied here, typically yield predictions with an accuracy of 75% to 80%. The large deviations between predicted and observed secondary structure for the α_2 , β_3 , and β_4 regions justify a further detailed inspection of these parts of the protein.

Figure 2 shows the per-residue scores of the two refined ensembles for four different WHAT IF quality indicators. The refined 1TGQ ensemble exhibits lower values for the packing quality [34] (see Figure 2A) compared to the refined 1Y4O

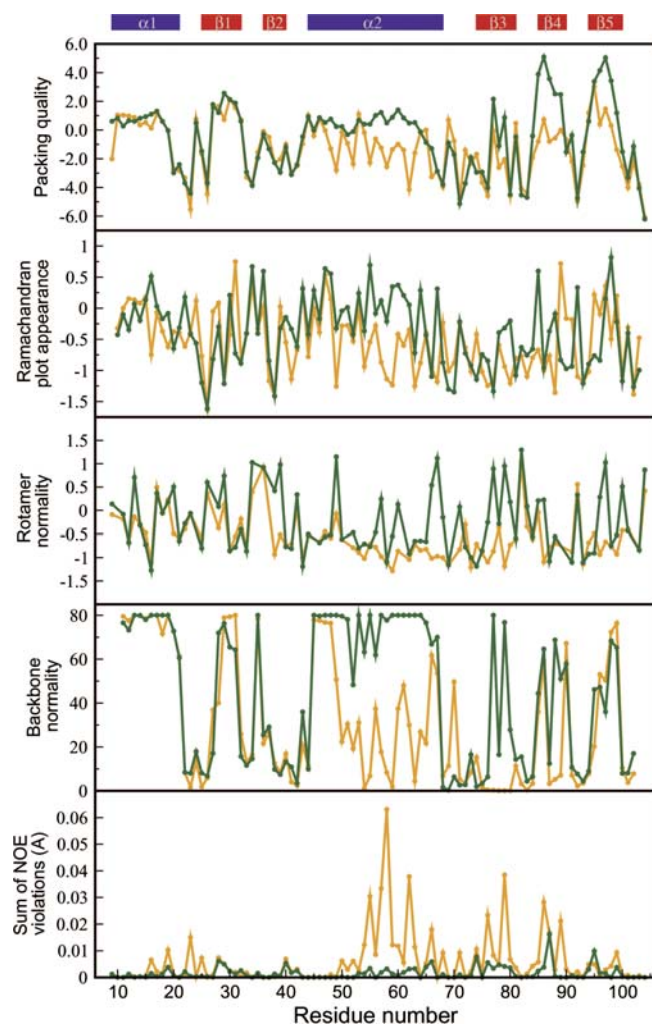


Figure 2. Five Different per-Residue Structural Quality Indicators

(A) Packing quality Z-score.

(B) Ramachandran plot appearance Z-score.

(C) Rotamer normality Z-score.

(D) Backbone normality score. The values listed on the y-axis indicate the number of times the local backbone (defined by the current residue plus or minus two residues) was found in WHAT IF's internal database (with a cut-off on the number of hits at 80).

(E) Sum of the NOE violations. Scores for the refined 1Y40 ensemble are shown in green; those for the refined 1TGQ ensemble are shown in orange. Secondary structure of the 1Y40 ensemble is indicated using colored boxes: α -helices are shown in blue, β -strands are shown in red. DOI: 10.1371/journal.pcbi.0020009.g002

ensemble, most notably in the $\alpha 2$, $\beta 4$, and $\beta 5$ regions. When the packing quality scores of 1TGQ are evaluated by themselves, the problematic regions do not particularly stand out. The same notion holds for the rotamer normality Z-scores (see Figure 2C), although the continuous stretch of residues from Pro45 to Arg80 with relatively low-quality scores should be considered suspicious. This is also expressed in the lower overall rotamer normality score, as already shown in Table 1. A nearly identical stretch of low scoring residues (from Met55 to Ile85) is observed when evaluating the Ramachandran plot quality scores (see Figure 2B). The finding that similar regions of consecutively low scoring residues are highlighted by different quality indicators provides more circumstantial evidence of the underlying problems, but again, no exceptional outliers are found.

Our analysis shows that only the backbone normality score unambiguously identifies the erroneous regions in the 1TGQ structure ensemble. Figure 2D shows the number of occurrences of the local backbone conformation of each residue in WHAT IF's nonredundant internal database. For NMR structures, it is quite common to find low backbone normality scores in loops and other flexible regions, as evidenced by the validation results of the 1Y40 ensemble where most low scoring regions are found between the different secondary structure elements. These low scoring loops do, however, not influence the overall backbone normality score, which for the 1Y40 structures falls well within the normal range (Table 1).

Regular secondary structure elements, such as α -helices, typically score very well on the backbone normality check (e.g., the $\alpha 1$ region in both ensembles and the $\alpha 2$ region of 1Y40). In the 1TGQ ensemble, however, unusually low backbone normality scores are observed for most residues in the $\alpha 2$ region. A near-zero number of hits is obtained for several residues (e.g., Met54, His55, Leu59, and Ser63), most of which are involved in bending the $\alpha 2$ -helix. Alarming are the successive residues Thr75-Arg80, which all have a backbone occurrence score of 0, indicating that no similar backbone conformations are observed in the WHAT IF internal database of high-quality crystal structures [35]. This is not uncommon for occasional residues in loops but highly unlikely for consecutive residues in a well-defined region of the structure and is indicative of either a very unique or a very wrong backbone conformation. In either case, these results indisputably warrant an in-depth investigation of these regions of the structure and the experimental data that define them.

To assess if the experimental data also indicate the same regions as problematic, the sum of the NOE violations per residue is shown in Figure 2E. The found violations are small and would under normal circumstances not be considered problematic, but again they are clustered in the $\alpha 2/\beta 3$ region. To further investigate this finding, we also analyzed the dataset constructed for the 1TGQ ensemble using the QUEEN program [36]. Using a representation of the structure in distance space and concepts derived from information theory, QUEEN can quantify the information contained in both individual restraints and sets of restraints. For the 1TGQ dataset, the total information content (I_{total}) and, for each of the individual restraints, the unique information content (I_{uni}) and the average information content (I_{ave}) were determined. We previously showed that combining the unique and average information content can be very useful in the identification of problematic restraints in an experimental dataset [36]. The $[I_{uni}, I_{ave}]$ plot shown in Figure 3 clearly illustrates the varying information content of the different restraints in the 1TGQ dataset. Similar to previous work [37], we evaluated the 30 most important and most informative restraints, all located above the dashed line in Figure 3. In total, 13 of the 30 most crucial restraints (indicated by the black squares in Figure 3) are located in regions of the structure ensemble that score low on the backbone normality check. As such, an analysis of the 1TGQ dataset using QUEEN would also have highlighted the $\alpha 2$ and $\beta 3$ regions as parts of the molecule deserving further investigation.

In summary, our analyses of both the structure ensemble and the supposedly observed experimental data of PDB entry 1TGQ clearly reveal the erroneous regions present in this set of

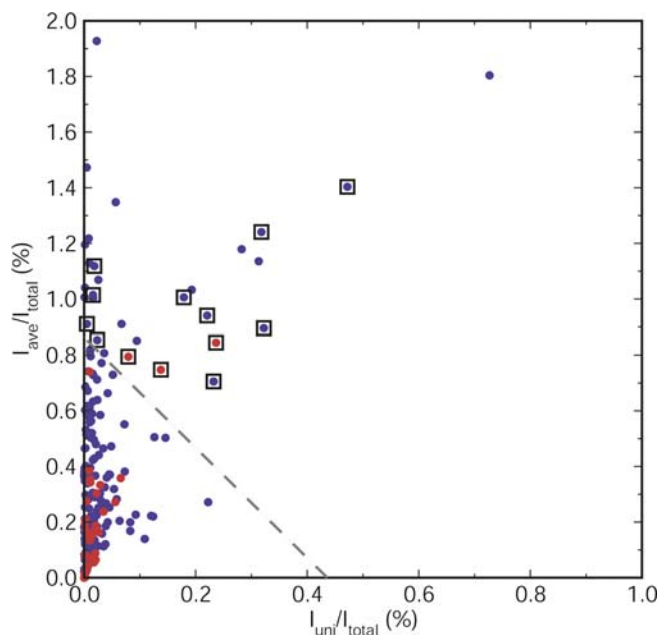


Figure 3. $[l_{uni}/l_{ave}]$ Plot for 1TGQ Calculated Using the QUEEN Program [36]

Long-range restraints (blue filled circles) and the 1TGQ_{sim} restraints (red filled circles) are indicated. Restraints that are among the 30 most unique and most important (those above the dashed gray line) and that involve residues in either the $\alpha 2$ or $\beta 3$ region (cf. Figure 1A) are indicated by black boxes.

DOI: 10.1371/journal.pcbi.0020009.g003

structural models. Such a severe error therefore should not have gone undiscovered in any structure determination project.

Evaluation of a Large Set of Recent NMR Structures

The fact that the erroneous 1TGQ ensemble made it into the PDB inevitably raises the question if more comparatively large errors might have gone unnoticed. To answer this question, we performed a quality analysis of a large set of protein NMR structures, the results of which are shown in Figure 4. The presented dataset was constructed by selecting from the PDB all NMR structures that were deposited after January 2003, consisted of at least 45 amino acids, and had more than 40% of their amino acids involved in secondary structure elements. The latter criterion was imposed to remove the models of largely unfolded structures that might bias our analysis. From this set all structural genomics target were filtered (310 in total), their quality scores are shown in orange in Figure 4. From the remaining NMR structures, originating from individual structure determination laboratories, an equally sized random selection of structures was made, whose quality scores are shown in green in Figure 4. For comparison, the average quality scores of the 1TGQ ensemble, both before and after refinement, are also indicated.

The data show no significant difference between the distributions of the quality indicators of structural genomics structures compared to those structures originating from individual research groups. In general, the distribution of the quality scores appears to be somewhat narrower for the structural genomics structures, but the average scores are similar, a result in-line with recent other studies [38]. Surprisingly, for both the packing and Ramachandran plot quality scores, the 1TGQ ensembles score comparable to the

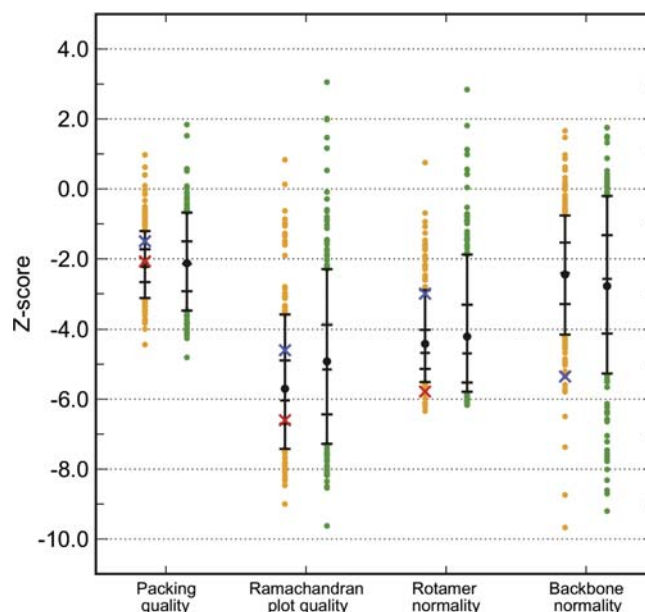


Figure 4. Structure Quality Z-Scores for a Large Set of Recent NMR Structures

The quality scores of 620 NMR ensembles released from the PDB after January 1, 2003, are shown. For comparison, the dataset is separated in structures solved as part of structural genomics projects (orange) and structures originating from individual research groups (green). For each quality indicator, the average Z-score is indicated with a filled black circle. The black horizontal markers indicate (from top to bottom) the 90th, 75th, 50th (the median), 25th, and 10th percentiles of the data points for each quality indicator. The distribution of the outliers outside the markers is indicated using colored data points. The quality scores of the original and refined 1TGQ ensemble (cf. Table 1) are indicated by red and blue crosses, respectively. The backbone normality score of 1TGQ is identical for the original and refined ensemble.

DOI: 10.1371/journal.pcbi.0020009.g004

majority of the NMR structures. The rotamer normality score initially places the 1TGQ ensemble among the 10% worst scoring structural genomics structures, but after refinement it is amidst the top 10%. As before, the backbone normality score consistently identifies the erroneous 1TGQ structures as one of the outliers. Given the serious errors present in the 1TGQ ensemble, one might consider the fact that several NMR structures solved over the past years demonstrate backbone normality scores lower than those of 1TGQ rather worrisome.

Visual inspection of the structural ensembles exhibiting lower backbone normality scores than 1TGQ revealed that in some instances these low scores resulted from the corresponding proteins exhibiting unusual folds or dynamic behavior. For others, however, we noted some striking structural abnormalities of which we will discuss two examples. First, our attention was drawn to the NMR structure with the lowest backbone normality Z-score ($Z = -9.8$). It corresponds to an alternatively spliced PDZ domain of PTP-Bas [39] (PDZ-Bas, PDB entry 1Q7X), which was determined in the context of the Structural Proteomics In Europe project (SPINE, <http://www.spineurope.org>). In this structure ensemble, an arginine side chain deeply penetrates the hydrophobic core (cf. Figure 5A). Arginine, however, is a very hydrophilic residue and is typically not observed in hydrophobic environments. In the highly identical alternative spliced second PDZ domain of PTP-BL [37] (PDZ-BL, PDB entry 1OZI, sequence identity 95% with PDB entry 1Q7X)

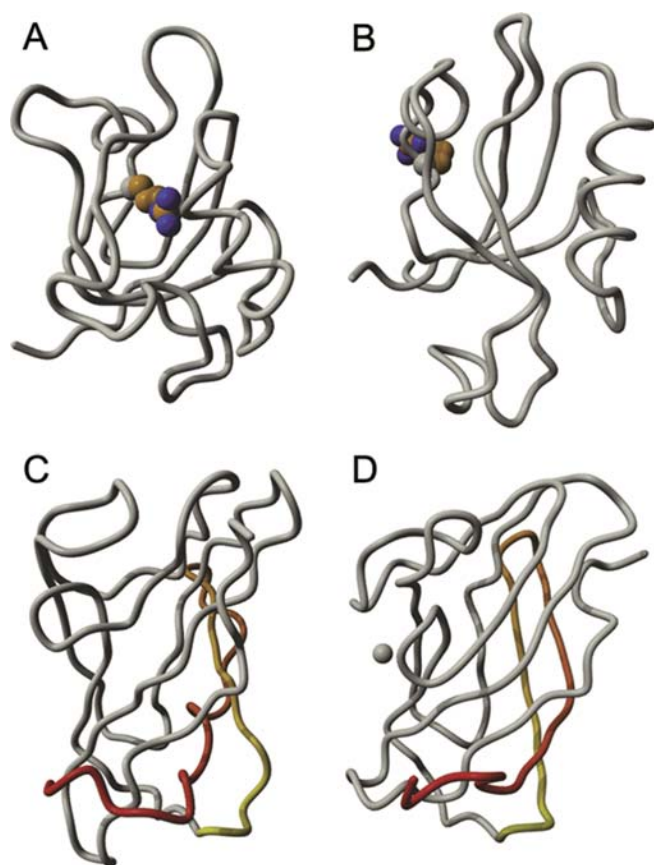


Figure 5. Examples of Observed Structural Anomalies

(A) An arginine side chain protruding the hydrophobic core of the second PDZ domain of PTP-Bas [39].

(B) The corresponding arginine in the highly homologous second PDZ domain of PTP-BL [37] is solvent exposed.

(C) The C-terminal region of DR1885 [42] (residues 120 to 149 are color-coded from yellow to red) forms a knot-like structure in the apo-form of DR1885.

(D) In the copper bound form of DR1885, the C-terminus wraps around the protein, instead of traversing through it. For each of the four structure ensembles, only the first, and presumably best, model is shown.

DOI: 10.1371/journal.pcbi.0020009.g005

and, to the best of our knowledge, in all other homologous PDZ domains, the corresponding arginine is indeed solvent exposed (cf. Figure 5B), rendering it very unlikely for the 1Q7X ensemble to be correct. This finding is corroborated by the backbone residual dipolar coupling (RDC) data [40] measured for the PDZ-BL protein [37]. To allow for a fair comparison, an ensemble of 20 PDZ-BL structures was calculated and refined using only the experimental distance and dihedral data and the procedures described above, as the deposited structures [37] were refined against the RDC restraints. The RDC R-factor [41] obtained for the newly calculated PDZ-BL ensemble is 43%, whereas the RDC R-factor of 69% for the PDZ-BAS ensemble is significantly higher. This clearly demonstrates the ability of RDC-derived orientational restraints to also distinguish incorrect backbone orientations, but unfortunately these data are typically not acquired in structural genomics pipelines.

As a second example, we noticed striking differences between the apo- and copper bound forms of the protein DR1885 [42] (PDB entries 1X7L and 1X9L), also originating

from the SPINE project. Most notable are the differences in the conformation of the C-terminal region of the protein (residues 120 to 149, Figure 5C and 5D). In the apo-form these residues are in a very unusual knot-like conformation, with the C-terminus passing through a loop consisting of residues 118 to 125. In the copper bound structures, the backbone of the C-terminal residues assumes a much more normal conformation and wraps around the DR1885 protein, instead of traversing through it. Given that there are no significant changes in the chemical shifts of the residues involved upon binding of copper to DR1885 (see Figure 2C in [42]), one of the two structure ensembles is almost certain to be incorrect.

In the publications describing the DR1885 protein [42] and the alternatively spliced PDZ domain from PTP-Bas [39], structural quality is foremost assessed by the number and size of the restraint violations and PROCHECK Ramachandran plot statistics. Our findings for the DLC2A protein already illustrated that these quality indicators are relatively insensitive to large structural errors, a result corroborated by the relatively acceptable scores found for these two datasets. Therefore, these examples clearly illustrate that the fact that no distance or dihedral angle violations are observed above a given threshold and that majority of the residues are found in allowed regions of the Ramachandran can be indicative of a good structure but does not provide any guarantees. It is interesting to note here that the three erroneous structures described in this paper stem from premier protein NMR groups, all involved in the development of structure validation and refinement methodologies [43–46], and that these methodologies either failed or were not or incorrectly applied in identifying the serious errors present in these structure ensembles.

To hopefully prevent such large errors from reoccurring in the future, we strongly suggest that validation results from normality checks, such as those implemented in the WHAT IF program [4,30], should be evaluated (and reported on) in any structure determination project. For high-throughput structural genomics projects, the application of multiple and sophisticated validation tools is even more critical, as much effort is geared towards minimizing the amount of expert time required for the determination and refinement of NMR structures [47]. Since this amount is deliberately continuously reduced, we expect structural genomics projects to become increasingly dependent on data and structure validation software to direct the spectroscopist to the regions that warrant his or her expert assessment.

Conclusions

We have shown that, when using only distance and dihedral restraints, even a largely incorrect structure is readily refined to seemingly acceptable levels of quality. As a result, the quality of biomolecular NMR structures cannot be safely assessed by the size and number of residual restraints violations, the precision of the structure ensemble, or even the fact that most residues are located in the allowed regions of the Ramachandran plot. Relying solely on these indicators to evaluate an ensemble of NMR structures therefore provides a false sense of correctness. The fundamentally different nature of residual dipolar couplings renders them complementary to traditional NMR data and a powerful tool to identify large errors in NMR structures. Unfortunately, in

many instances, such as in most structural genomics efforts, they are not routinely acquired and proper use of structure validation tools then becomes crucial. Furthermore, our results show that also more sophisticated quality indicators, e.g., the overall WHAT IF backbone normality score, do not unambiguously identify problematic structures. In contrast, we showed that only the simultaneous evaluation of multiple quality indicators on a per-residue basis, however, combined with a careful evaluation of the experimental data (e.g., using QUEEN), does allow for the well-supported identification erroneous regions in biomolecular NMR structures, thereby avoiding errors as those reported here.

Materials and Methods

NMR structures and data. For both mDLC2A and hDLC2A, the structure ensembles were obtained from the PDB (PDB entries 1Y4O and 1TGQ, respectively). The residue numbering of the 1TGQ ensemble was adjusted to match to that of the 1Y4O ensemble, as shown in Figure 1. The coordinates describing the His-tag in the 1Y4O ensemble (residues 1 to 8) were removed so that all DLC2A models contained an equal number of residues.

The experimental restraints for the 1Y4O ensemble, solved as a dimer, were obtained from the PDB, for the 1TGQ ensemble no experimental restraints were available at the time of writing. All stereospecifically assigned NOEs were deassigned for the violation analyses, structure calculations, and refinements. To be able to apply the same dataset to both structures, all restraints involving unique atoms of the three amino acids that are different in both sequences (cf. Figure 1A and 1B) were removed from the dataset. The final dataset contained 1,395 distance restraints, consisting of 553 intraresidue, 341 sequential, 278 medium-range, 187 long-range, and 72 intermolecular restraints. In addition, 146 dihedral angle

restraints were included in all refinements. The deposited dataset also contained 96 hydrogen bond restraints, but as it is not clear how these were derived, and as they showed considerable violations in the deposited 1Y4O ensemble, these restraints were excluded from all analyses.

Structure calculation and refinement protocols. All structure calculations were performed using CNS [48] and the default simulated annealing protocol, as provided with the software package. All refinements in explicit solvent [7] were performed using XPLOR-NIH [49] using the refinement procedure as described before [8]. Both the deposited and newly generated structure ensembles were validated using PROCHECK [29] and WHAT IF [30]. The deposited and constructed datasets were evaluated using the QUEEN program [36].

Supporting Information

Accession Numbers

The UniProt (Universal Protein Resource) (<http://www.pir.uniprot.org>) accession numbers for mDLC2A and hDLC2A are P62627 and Q9NP97, respectively.

Acknowledgments

Author contributions. SBN, CAEMS, GWV, and GV conceived and designed the experiments. SBN performed the experiments. SBN and CAEMS analyzed the data. SBN wrote the paper.

Funding. The authors acknowledge financial support from the EMBRACE project funded by the European Commission (contract LHSG-CT-2004-512092) and the BioRange program of the Netherlands Bioinformatics Centre, which is supported by a BSIK grant through the Netherlands Genomics Initiative.

Competing interests. The authors have declared that no competing interests exist. ■

References

- Kleywegt GJ (2000) Validation of protein crystal structures. *Acta Crystallogr D* 56: 249–265.
- DePristo MA, de Bakker PI, Blundell TL (2004) Heterogeneity and inaccuracy in protein structures solved by X-ray crystallography. *Structure (Camb)* 12: 831–838.
- Branden CI, Jones TA (1990) Between objectivity and subjectivity. *Nature* 343: 687–689.
- Hoofst RW, Vriend G, Sander C, Abola EE (1996) Errors in protein structures. *Nature* 381: 272.
- Doreleijers JF, Rullmann JA, Kaptein R (1998) Quality assessment of NMR structures: A statistical survey. *J Mol Biol* 281: 149–164.
- Spronk CA, Linge JP, Hilbers CW, Vuister GW (2002) Improving the quality of protein structures derived by NMR spectroscopy. *J Biomol NMR* 22: 281–289.
- Linge JP, Williams MA, Spronk CA, Bonvin AM, Nilges M (2003) Refinement of protein structures in explicit solvent. *Proteins* 50: 496–506.
- Nabuurs SB, Nederveen AJ, Vranken W, Doreleijers JF, Bonvin AM, et al. (2004) DRESS: A Database of REfined Solution nmr Structures. *Proteins* 55: 483–486.
- Berman HM, Westbrook J, Feng Z, Gilliland G, Bhat TN, et al. (2000) The Protein Data Bank. *Nucleic Acids Res* 28: 235–242.
- McRee DE, Tainer JA, Meyer TE, Van Beeumen J, Cusanovich MA, et al. (1989) Crystallographic structure of a photoreceptor protein at 2.4 Å resolution. *Proc Natl Acad Sci U S A* 86: 6533–6537.
- Borgstahl GE, Williams DR, Getzoff ED (1995) 1.4-Å Structure of photoactive yellow protein, a cytosolic photoreceptor: Unusual fold, active site, and chromophore. *Biochemistry* 34: 6278–6287.
- Kelly JA, Knox JR, Moews PC, Hite GJ, Bartolone JB, et al. (1985) 2.8-Å Structure of penicillin-sensitive D-alanyl carboxypeptidase-transpeptidase from *Streptomyces* R61 and complexes with beta-lactams. *J Biol Chem* 260: 6449–6458.
- Kelly JA, Kuzin AP (1995) The refined crystallographic structure of a DD-peptidase penicillin-target enzyme at 1.6 Å resolution. *J Mol Biol* 254: 223–236.
- Clore GM, Omichinski JG, Sakaguchi K, Zambrano N, Sakamoto H, et al. (1994) High-resolution structure of the oligomerization domain of p53 by multidimensional NMR. *Science* 265: 386–391.
- Jeffrey PD, Gorina S, Pavletich NP (1995) Crystal structure of the tetramerization domain of the p53 tumor suppressor at 1.7 Å resolution. *Science* 267: 1498–1502.
- Clore GM, Omichinski JG, Sakaguchi K, Zambrano N, Sakamoto H, et al. (1995) Interhelical angles in the solution structure of the oligomerization domain of p53: Correction. *Science* 267: 1515–1516.
- Lambert LJ, Schirf V, Demeler B, Cadene M, Werner MH (2001) Flipping a genetic switch by subunit exchange. *EMBO J* 20: 7149–7159.
- Urbauer JL, Simeonov MF, Urbauer RJ, Adelman K, Gilmore JM, et al. (2002) Solution structure and stability of the anti-sigma factor AsiA: Implications for novel functions. *Proc Natl Acad Sci U S A* 99: 1831–1835.
- Lambert LJ, Schirf V, Demeler B, Cadene M, Werner MH (2004) Flipping a genetic switch by subunit exchange. *EMBO J* 23: 3186.
- Altschul SF, Madden TL, Schaffer AA, Zhang J, Zhang Z, et al. (1997) Gapped BLAST and PSI-BLAST: A new generation of protein database search programs. *Nucleic Acids Res* 25: 3389–3402.
- Chothia C, Lesk AM (1986) The relation between the divergence of sequence and structure in proteins. *EMBO J* 5: 823–826.
- Sander C, Schneider R (1991) Database of homology-derived protein structures and the structural meaning of sequence alignment. *Proteins* 9: 56–68.
- Rost B (1999) Twilight zone of protein sequence alignments. *Prot Eng* 12: 85–94.
- Montelione GT, Zheng D, Huang YJ, Gunsalus KC, Szyperski T (2000) Protein NMR spectroscopy in structural genomics. *Nat Struct Biol* 7 (Suppl): 982–985.
- Bodenhausen G, Ruben DJ (1980) Natural abundance N-15 NMR by enhanced heteronuclear spectroscopy. *Chem Phys Lett* 69: 185–189.
- Anglister J, Grzesiek S, Ren H, Klee CB, Bax A (1993) Isotope-edited multidimensional NMR of calcineurin B in the presence of the non-deuterated detergent CHAPS. *J Biomol NMR* 3: 121–126.
- Burgering MJ, Boelens R, Caffrey M, Breg JN, Kaptein R (1993) Observation of inter-subunit nuclear Overhauser effects in a dimeric protein. Application to the Arc repressor. *FEBS Lett* 330: 105–109.
- Ilangovan U, Ding W, Zhong Y, Wilson CL, Groppe JC, et al. (2005) Structure and dynamics of the homodimeric dynein light chain km23. *J Mol Biol* 352: 338–354.
- Laskowski RA, MacArthur MW, Moss DS, Thornton JM (1993) PROCHECK: A program to check the stereochemical quality of protein structures. *J Appl Cryst* 26: 283–291.
- Vriend G (1990) . Vriend G (1990) WHAT IF: A molecular modeling and drug design program. *J Mol Graph* 8: 52–56, 29.
- Hoofst RW, Sander C, Vriend G (1997) Objectively judging the quality of a protein structure from a Ramachandran plot. *Comp Appl Biosci* 13: 425–430.
- Spronk CA, Nabuurs SB, Krieger E, Vriend G, Vuister GW (2004) Validation of protein structures derived by NMR spectroscopy. *Prog Nucl Magn Reson Spectrosc* 45: 315–337.
- Jones DT (1999) Protein secondary structure prediction based on position-specific scoring matrices. *J Mol Biol* 292: 195–202.

34. Vriend G, Sander C (1993) Quality control of protein models: Directional atomic contact analysis. *J Appl Cryst* 26: 47–60.
35. Hoofst RWW, Sander C, Vriend G (1996) Verification of protein structures: Side-chain planarity. *J Appl Cryst* 29: 714–716.
36. Nabuurs SB, Spronk CA, Krieger E, Maassen H, Vriend G, et al. (2003) Quantitative evaluation of experimental NMR restraints. *J Am Chem Soc* 125: 12026–12034.
37. Walma T, Aelen J, Nabuurs SB, Oostendorp M, van den Berk L, et al. (2004) A closed binding pocket and global destabilization modify the binding properties of an alternatively spliced form of the second PDZ domain of PTP-BL. *Structure (Camb)* 12: 11–20.
38. Snyder DA, Bhattacharya A, Huang YJ, Montelione GT (2005) Assessing precision and accuracy of protein structures derived from NMR data. *Proteins* 59: 655–661.
39. Kachel N, Erdmann KS, Kremer W, Wolff P, Gronwald W, et al. (2003) Structure determination and ligand interactions of the PDZ2b domain of PTP-Bas (hPTP1E): splicing-induced modulation of ligand specificity. *J Mol Biol* 334: 143–155.
40. Tjandra N, Bax A (1997) Direct measurement of distances and angles in biomolecules by NMR in a dilute liquid crystalline medium. *Science* 278: 1111–1114.
41. Clore GM, Garrett DS (1999) R-factor, free R, and complete cross-validation for dipolar coupling refinement of NMR structures. *J Am Chem Soc* 121: 9008–9012.
42. Banci L, Bertini I, Ciofi-Baffoni S, Katsari E, Katsaros N, et al. (2005) A copper(I) protein possibly involved in the assembly of CuA center of bacterial cytochrome c oxidase. *Proc Natl Acad Sci U S A* 102: 3994–3999.
43. Gronwald W, Kirchhofer R, Gorler A, Kremer W, Ganslmeier B, et al. (2000) RFAC, a program for automated NMR R-factor estimation. *J Biomol NMR* 17: 137–151.
44. Bertini I, Cavallaro G, Luchinat C, Poli I (2003) A use of Ramachandran potentials in protein solution structure determinations. *J Biomol NMR* 26: 355–366.
45. Huang YJ, Moseley HN, Baran MC, Arrowsmith C, Powers R, et al. (2005) An integrated platform for automated analysis of protein NMR structures. *Methods Enzymol* 394: 111–141.
46. Huang YJ, Powers R, Montelione GT (2005) Protein NMR recall, precision, and F-measure scores (RPF scores): Structure quality assessment measures based on information retrieval statistics. *J Am Chem Soc* 127: 1665–1674.
47. Liu G, Shen Y, Atreya HS, Parish D, Shao Y, et al. (2005) NMR data collection and analysis protocol for high-throughput protein structure determination. *Proc Natl Acad Sci U S A* 102: 10487–10492.
48. Brünger AT, Adams PD, Clore GM, Delano WL, Gros P, et al. (1998) Crystallography and NMR system (CNS): A new software system for macromolecular structure determination. *Acta Cryst D* 54: 905–921.
49. Schwieters CD, Kuszewski JJ, Tjandra N, Marius Clore G (2003) The Xplor-NIH NMR molecular structure determination package. *J Magn Reson* 160: 65–73.
50. McGuffin LJ, Bryson K, Jones DT (2000) The PSIPRED protein structure prediction server. *Bioinformatics* 16: 404–405.